JKGS *Journal of the Korean GNSS Society*

Performance Analysis of Pseudolite Tropospheric Delay Models Using Radiosonde Meteorological Data

Hyoungmin So, Junpyo Park[†], Kiwon Song
Agency for Defense Development, Yuseong P.O. Box 35-3, Daejeon 305-600, Korea

ABSTRACT

When pseudolite navigation system is applied to wide area, the tropospheric delay is the main error factor. In this study, we experimentally compared and analyzed the performance of the conventional pseudolite tropospheric delay models. The integration method using radiosonde meteorological data was suggested to derive the reference value for the comparison and analysis. Flight tests were carried out to analyze the performance of the tropospheric delay models according to the elevation angle and distance conditions between the user receiver and the pseudolite. As the results of this study, we provided the basis for the choice of tropospheric delay model appropriate to the relative location characteristics of the pseudolite and the user.

Keywords: tropospheric delay, radiosonde, pseudolite, GNSS, navigation

1. INTRODUCTION

The error factors of satellite navigation system include the satellite orbit error, satellite clock error, ionospheric delay error, tropospheric delay error, and receiver-related error. Among these various error factors, the tropospheric delay error has a weaker effect than that of the major error factors such as the satellite-related error and ionospheric delay error, because the tropospheric delay error is effectively corrected thanks to various tropospheric delay models that have already been developed and are applicable to satellite navigation. It is estimated that the tropospheric delay error is about 0.2m (1σ) in the GPS pseudorange error in the U.S (Kaplan & Hegarty 2006).

A pseudolite, which is the instrument that transmits the navigation signals that are similar to those of the Global Navigation Satellite System (GNSS), is established in the GNSS shaded areas to improve navigation performance and availability of GNSS or to be used as a GNSS-independent navigation system (Kee et al. 2003). When a pseudolite

is installed indoors and operated as a single navigation system or used within a limited range, the error caused by tropospheric delay is not significantly taken into account (So et al. 2010). On the contrary, in the pseudolite navigation that is operated in a relatively wide area as in aircraft take-off and landing, the tropospheric delay error should be corrected. A pseudolite is usually installed on the ground, and thus the accurate position can be measured by precise positioning, and it is not changed once it is accurate measured. Therefore, the pseudolite position error is relatively small compared with the GNSS satellite orbit error. Additionally, signal transmission and reception are performed within lower altitude, and thus the ionospheric delay error is not taken into account. In the pseudolite navigation system, while the importance of the satellite-related error and the ionospheric delay error, the major GNSS error factors, is decreased, the tropospheric delay error must be considered significantly. This is because the magnitude of the tropospheric delay error is increased in proportion to the distance between the pseudolite and user receiver. The recent flight experiment by Locata, Australia, identified the tropospheric delay error as a major error factor, though it had not been significantly considered in the conventional satellite navigation (Craig & Locata Corp. 2012).

The tropospheric delay model that is used in the conventional satellite navigation cannot be directly applied to the estimation of the tropospheric delay in the pseudolite navigation system. Because the pseudolite signal transmission path is horizontal in the lower troposphere, the tropospheric delay estimation is very difficult (Wang et al. 2005). Therefore, the tropospheric delay models applicable to pseudolite have been developed on the basis of the tropospheric delay models applied to the conventional satellite navigation system.

According to (Wang et al. 2005), the tropospheric delay estimation methods applicable to the pseudolite navigation system are classified into three categories: the integration method, the difference method using a mapping function, and the distance proportion method. In the integration method, the refractivity of the atmosphere is modeled according to the altitude on the basis of empirical data and then it is integrated along the signal transduction path between the pseudolite and the user. The Radio Technical Commission for Aeronautics (RTCA) model and the Hopfield model are based on the method. In the difference method using a mapping function, a virtual GNSS satellite is assumed, the tropospheric delay between the virtual GNSS satellite and the pseudolite as well as the tropospheric delay between the virtual GNSS satellite and the receiver is calculated by the mapping function, and then the tropospheric delay between the pseudolite and the user receiver is estimated. Neill Mapping Function and Saastamoinen model have been applied as a mapping function for the difference method. In the distance proportion method, it is assumed that the tropospheric delay is simply proportional to the distance between the pseudolite and the user receiver.

The main objective of this study was to compare the performance the tropospheric delay estimation methods that have already been suggested. Even though various methods have been suggested, their performance has been rarely compared and analyzed experimentally. The most important thing in analyzing the performance of various models is how to calculate the reference tropospheric delay. In this study, we suggested the path integration method using radiosonde meteorological observation data. And the result was used as the reference for comparison. Navigation coverage within about a 50 km-radius was assumed. A flight test using an aircraft was carried out to compare the performance.

This article is composed of five chapters. Chapter 2 briefly reviews the conventional tropospheric delay estimation methods. Chapter 3 introduces the path integration method using a radiosonde. Chapter 4 shows experimental results and compares them with that of the conventional method in term of performance. Chapter 5 concludes the article and discusses future issues.

2. REVIEW OF PREVIOUS WORKS

As mentioned above, the conventional methods to estimate the pseudolite tropospheric delay error are classified into three categories. Since we assume a code-based standalone navigation in the environment composed of a ground pseudolite and a user in the air located within a 50-km radius, we briefly introduce the method based on the RTCA model and the Hopfield model and the difference method based on the Saastamoinen model, excluding the distance proportional method.

2.1 RTCA model

The RTCA model, which was proposed in order to apply to the pseudolite used for take-off and landing of aircraft in airports, is defined in the document RTCA DO-246A (RTCA 2000). Eq. (1) shows the RTCA model equation:

$$\delta R_{Tr} = N_{APL} \times \left(1 - \Delta h_u / h_0\right) \times R \times 10^{-6} \tag{1}$$

δR_{Tr} : tropospheric delay
N_{APL} : tropospheric refractivity along the signal path
Δh_u : altitude of the user relative to the APL
h_0 : scale height
R : range between the APL and the user

For dry and wet atmosphere, the scale height and refractivity are respectively applied to calculate the dry delay and wet delay, and their sum is determined as the total tropospheric delay. According to the simulation results of a conventional study, the RTCA model seems to be appropriate when the distance between the user and the pseudolite is short and the height is not much different (Wang et al. 2005). This may be because the effect of height difference and distance has been modeled as a first order in the RTCA model as it was developed primarily for the modeling of aircraft take-off and landing in the airports.

The modified RTCA model, in which the height difference is considered more importantly than in the RTCA model, has been proposed by handling the height difference as a second order (Biberger et al. 2003). However, showed that the simulation result was similar to that of the RTCA model in the case where the height difference was great (Wang et

al. 2005). Eq. (2) shows the equation for the modified RTCA:

$$\Delta_{*,Trop} = 10^{-6} \cdot N_* \cdot D \cdot \left(1 - \frac{2(h_{ROV} - h_{APL})}{h_{*,0}} + \frac{2(h_{ROV}^2 + h_{ROV} h_{APL} + h_{APL}^2)}{h_{*,0}^2} \right) \quad (2)$$

$\Delta_{*,Trop}$: tropospheric delay
N_* : tropospheric refractivity
D : range between the APL and the user
$h_{*,0}$: scale height
h_{ROV} : height of rover
h_{APL} : height of APL

2.2 Hopfield model-based integration method

The Hopfield model deals with the refractivity of dry atmosphere along the vertical direction on the basis of the actual meteorological observation data (Hofmann-Wellenhof et al. 2000). Although the modeling is difficult for the wet atmosphere, the Hopfield model applies the same modeling method to the wet atmosphere. Eq. (3) shows the refractivity model as a function of height defined in the Hopfield model:

$$N_*^{Trop}(h) = N_{*,0}^{Trop} \left[\frac{h_* - h}{h_*} \right]^4 \quad (3)$$

N_*^{Trop} : refractivity
h : height
$N_{*,0}^{Trop}$: refractivity at surface
h_* : scale height

Eq. (3) is applied to both the dry and wet atmosphere, and the refractivity at the ground surface, N_*^{Trop}, and the height, h_*, should be applied for the dry and wet atmosphere, respectively. Since the Hopfield model defines the atmospheric refractivity in the vertical direction, the refractivity should be integrated along the actual signal transmission path to calculate the atmospheric delay, N_*^{Trop}. Eq. (4) shows the integration procedure:

$$\Delta_*^{Trop} = 10^{-6} N_{*,0}^{Trop} \int \left[\frac{h_* - h}{h_*} \right]^4 ds \quad (4)$$

Δ_*^{Trop} : refractivity
s : signal transmission path

The tropospheric delay based on the Hopfield model generally used in the GNSS is estimated by integrating Eq.

(4) in the vertical direction from the user receiver height to the scale height, estimating the tropospheric delay in the zenithal direction and then applying it to the mapping function to calculate the actual slant delay.

Bouska & Raquet (2003) proposed a pseudolite tropospheric delay model that seems to be based on the Hopfield model. Considering that the pseudolite is located on the ground, contrary to the GNSS satellite, and the user is located within the scale height range, the distance and the height difference between the pseudolite and the user receiver was reflected on the model. Eq. (5) shows the model equation:

$$\Delta_* = \frac{1}{5} \cdot 10^{-6} \cdot N_* \cdot R_u \cdot \frac{h_{*,0} - h_s}{\Delta h_u} \left[\left(1 - \frac{\Delta h_{APL}}{h_{*,0} - h_s} \right)^5 - \left(1 - \frac{\Delta h_{APL} + \Delta h_u}{h_{*,0} - h_s} \right)^5 \right] \quad (5)$$

Δ_* : tropospheric delay
R_u, R_R : slant range from pseudolite to user and ref. rcv., respectively
Δh_u : height of the user above the pseudolite
Δh_{APL} : height difference from pseudolites to ref. rcv.
$h_{*,0}$: scale height
h_s : height of reference receiver
N_* : surface refractivity

It is known that the Hopfield model is relatively stable toward the change in the distance and the elevation between the pseudolite and the user receiver. However, the need for additional tests in various conditions was mentioned because such an analysis was based on simulation and a specific flight test (Wang et al. 2005). Our study is aimed at the comparison and analysis of the methods with reference to radiosonde meteorological observation data.

2.3 Single difference method using Saastamoinen model

The mapping function difference method using the Saastamoinen model is to apply the model to a virtual GNSS satellite. To calculate the tropospheric delay between the pseudolite and the user receiver, a virtual GNSS satellite is assumed on the extension line of the pseudolite and the user receiver. The tropospheric delay between the pseudolite and the virtual GNSS satellite and that between the user receiver and the virtual GNSS satellite are estimated using the Saastamoinen model, and then, from the difference between them, the tropospheric delay is estimated (Wang et al. 2005).

The Saastamoinen model has been proposed to correct the conventional mapping function whose accuracy is

decreased as the elevation is low by adding a correctional term for the elevation angle of 10 to 30 degrees, a relatively low elevation range. Eq. (6) shows the modeling equation of the Saastamoinen model. The correctional term used in the model can be found in (Hofmann-Wellenhof et al. 2000).

$$\Delta_{Trop} = \frac{0.002277}{\cos Z}\left[P+\left(\frac{1255}{T}+0.05\right)\cdot e-B\cdot \tan^2 Z\right]+\delta R \quad (6)$$

Z : zenith angle
P : pressure
T : temperature
e : vapor pressure
B : correction term for height
δR : correction term for both height and zenith angle

In the previous studies where the Saastamoinen model was applied to a pseudolite, the performance decrease was revealed at the low elevation angles that are the limitations of the mapping function. Although the Saastamoinen model showed better results than those of other models when the elevation angle was high, a simulation showed that the model had a tendency that was significantly different from that of other models if the elevation angle was low (Wang et al. 2005).

3. CALCULATION OF TROPOSPHERIC DELAY WITH RADIOSONDE METEOROLOGICAL DATA

The conventional methods previously described employ the atmospheric refractivity model constituted on the basis of empirical data. Different from the signal transmission path characteristics in the satellite navigation system, however, the pseudolite navigation system has a longer horizontal signal transmission path and thus the tropospheric delay is even more difficult due to the drastically fluctuating meteorological conditions and the irregularity of the meteorological state (Wang et al. 2005). Therefore, if the standardized refractivity model is applied to the integration method, the error may be increased in proportion to the distance between the user receiver and the pseudolite. Additionally, it has been known that the mapping function used in the difference method has a low reliability in the low elevation angle environment (Kaplan & Hegarty 2006). Thus, the mapping function difference method may not be available in the pseudolite navigation system where the elevation angle is often low between the

pseudolite and the user receiver.

At this point, the need is raised to choose a model appropriate to specific application areas among the many conventional models. The optimum model should be chosen considering the pros and cons of each model and the characteristics depending on the relative arrangement of the pseudolite and the user receiver. This article suggests the tropospheric delay estimation method based on the radiosonde meteorological observation data in order to compare the performance of the conventional methods. Several assumptions were made for the suggested method, and the assumptions and calculation methods are explained below.

The tropospheric delay is calculated using the radiosonde meteorological observation data in the following procedure. Firstly, using the meteorological data such as temperature, atmospheric pressure and humidity measured along the height, the refractivity with respect to dry and wet atmosphere is computed as in Eqs. (7) and (8) (Hofmann-Wellenhof et al. 2000):

$$N_{dry} = 77.6\cdot \frac{P}{T} \quad (7)$$

P : atmospheric pressure
T : temperature

$$N_{wet} = 22770\cdot \frac{f}{T^2}\cdot 10^{\frac{7.4475(T-273)}{T-38.3}} \quad (8)$$

f : relative humidity

Assuming that the radiosonde meteorological observation data along the height are the same horizontally within a radius of 50 km, the refractivity in each interval is integrated by means of linear interpolation with respect to the path from the pseudolite and the user receiver to estimate the tropospheric delay. At this time, integration must be performed along the actual signal transmission path, not along the geometrical path that straightly links the pseudolite and the user receiver. Eq. (9) shows the integration formula with respect to the actual path:

$$\begin{aligned}\Delta Trop_{actual} &= \int_{actual}n(s)ds - \int_{actual}ds\\&= \int_{actual}[n(s)-1]ds\\&= 10^{-6}\int_{actual}N(s)ds\end{aligned} \quad (9)$$

n : refractive index
N : refractivity

The actual signal transmission path between the pseudolite and the user receiver used in Eq. (9) is not straight but curved with a certain curvature due to the change in the atmospheric refractivity on the transmission path. As we assumes a code-based single navigation user in this study, however, the tropospheric delay was calculated by assuming a straight path connecting the pseudolite and the user receiver, neglecting the delay caused by the refraction of the signal transmission path, as shown in Eq. (10):

$$\Delta Trop_{geometric} = 10^{-6} \int_{geometric} N(s)ds \quad (10)$$

The refractive model needed for the path integration was applied after linearly interpolating the radiosonde data, as shown in Fig. 1. In Fig. 1, the radiosonde meteorological observation data samples observed along the height were presented on the left side of the axis, and the transmission and reception straight path was presented on the right side along the axis which is the horizontal distance between the receiver and the transmitter. S (Tx) and S (Rx) denote the location of the pseudolite and the user receiver, respectively. $Slant$D denotes the slant distance between the pseudolite and the user receiver. The S axis is the path connecting the pseudolite and the user receiver. So, using the slant distance and the height difference between the pseudolite and the user receiver, the meteorological data acquired in the height direction can be applied to the path.

Fig. 2 schematically illustrates the linear refractive model for each interval with respect to the path connecting the transmitter and the receiver.

By defining the sample intervals with reference to the height at which the meteorological data were acquired, the partial tropospheric delay is calculated using the refractivity linearized in each interval and the tropospheric delay over the entire path can be computed by adding all the partial
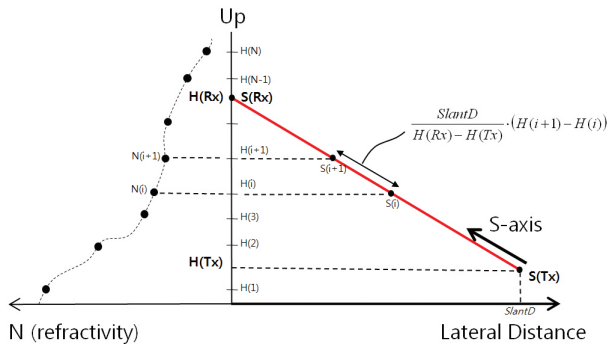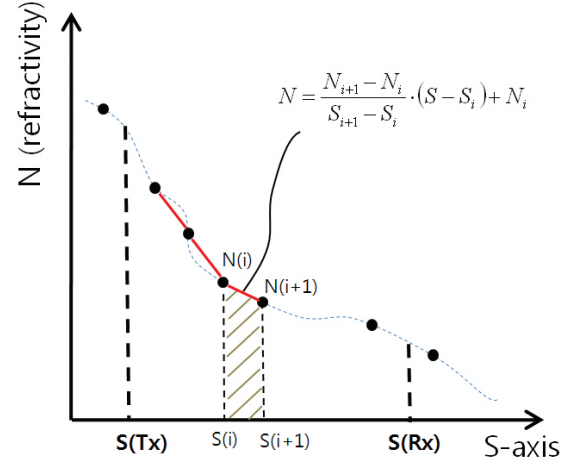

Fig. 2. Refractivity profile with respect to geometric signal path.

tropospheric estimations, as shown in Eq. (11):

$$TropoDelay = 10^{-6} \cdot \int_{S(Tx)}^{S(Rx)} N(s)ds = \sum_i \Delta TropoDelay(i) \quad (11)$$

The partial tropospheric delay in Eq. (11) is calculated as in Eq. (12):

$$
\begin{aligned}
\Delta TropoDelay(i) &= 10^{-6} \cdot \int_{s(i)}^{s(i+1)} N(s)ds \\
&= 10^{-6} \cdot \int_{s(i)}^{s(i+1)} \left[\frac{N(i+1)-N(i)}{S(i+1)-S(i)} \cdot (s-s(i)) + N(i) \right] ds \\
&= 10^{-6} \cdot (S(i+1)-S(i)) \cdot \frac{N(i)+N(i+1)}{2} \\
&= 10^{-6} \cdot \frac{SlantD}{H(Rx)-H(Tx)} \cdot (H(i+1)-H(i)) \cdot \frac{N(i)+N(i+1)}{2} \quad (12)
\end{aligned}
$$

4. FLIGHT TEST RESULTS

The performance of the conventional pseudolite tropospheric delay models was analyzed through a flight test. As described previously, the estimation results of the tropospheric delay based on the radiosonde data were employed as the reference values for the performance analysis. The flight test was carried out in the two flight paths schematically illustrated in Fig. 3. In the Case 1 scenario, the aircraft maintained a constant height and flied to the pseudolite transmitter. In this experiment, the elevation angle between the user receiver and the pseudolite was kept at a low level. In the Case 2 scenario, the aircraft flied to the transmitter, decreasing the height from a high height. In this case, the elevation angle between the user receiver and the pseudolite was kept at a relatively high level.
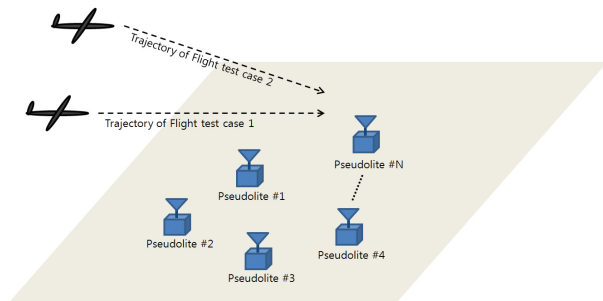

Fig. 1. Refractivity profile with respect to height (left axis) and 2-dimensional geometric signal path (right axis).

Fig. 3. Conceptual view of pseudolite navigation system with user trajectories and ground-installed pseudolites.
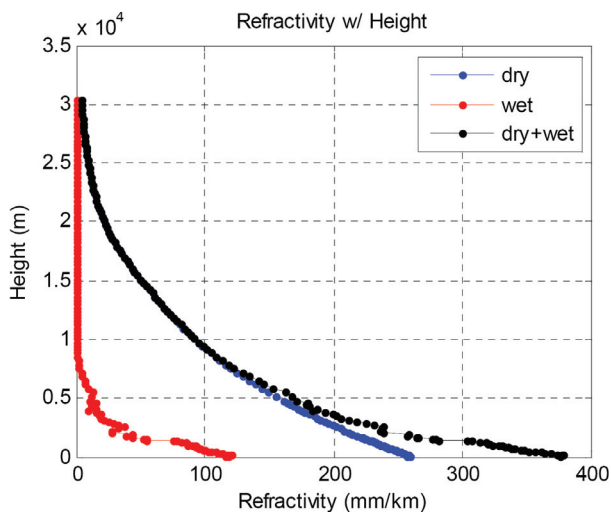

Fig. 4. Dry and wet refractivities calculated from radiosonde meteorological data.

4.1 Refractivity calculated from radiosonde meteorological data

Firstly, we performed radiosonde meteorological observation in advance of each flight test. Fig. 4 shows the dry and wet atmospheric refractivity calculated by applying Eqs. (7) and (8) with the radiosonde observation data and the total refractivity calculated by adding the dry and wet atmospheric refractivity together.

4.2 Flight test case 1

Fig. 5 shows the tropospheric delay estimation result of the flight test Case 1. The tropospheric delay estimation result of each model was shown over time, and the trend of the elevation angle and distance between the pseudolite and the user receiver was shown, too. The relative distance was gradually decreased, while the elevation angle was gradually increased, because the aircraft flied to the transmitter maintaining a constant height in the Case 1
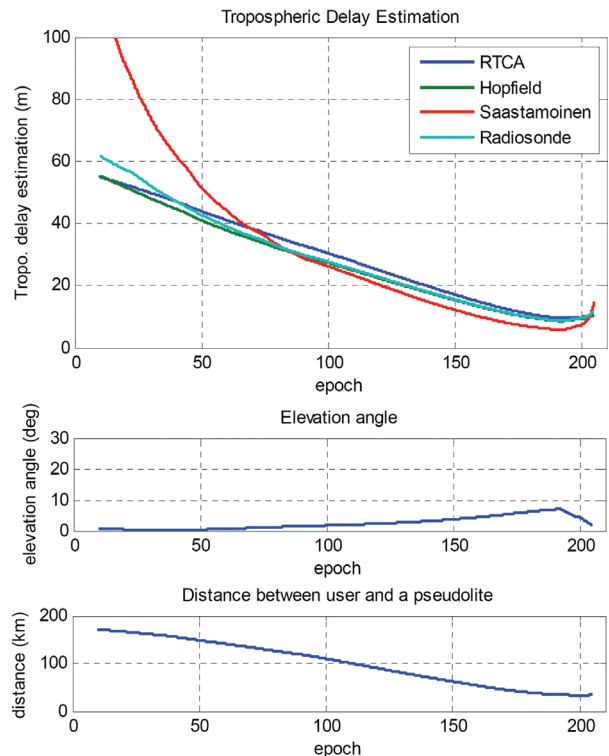

Fig. 5. Tropospheric delay estimation results of flight test case 1 (top: tropospheric delay estimation, middle: elevation angle between user and pseudolite, bottom: distance between user and pseudolite).

flight test. One feature of this test is that the Saastamoinen model-based difference method showed a trend that was significantly different from that of other models as well as the radiosonde-based model when the elevation angle was very low in the range of the epoch No. 50 or less. This indicates the limit of general mapping functions: the reliability of a mapping function is decreased when the elevation angle is low. In the range of the epoch No. 200 or more, the Saastamoinen model showed a drastic difference with the other models as the elevation angle was lowered again. It was also found that other models showed the same trend with that of the radiosonde data-based method.

4.3 Flight test case 2

The result of the Case 2 flight test, presented in Fig. 6, shows that the elevation angle between the pseudolite and the user receiver was kept sufficiently high while the relative distance was gradually reduced. From the epoch No. 70 to No. 90, the conventional methods, except the Saastamoinen model, showed a significant difference with the radiosonde-based method. This may be mainly because the Hopfield model and the RTCA model are derived by integration and the height difference between the pseudolite and the
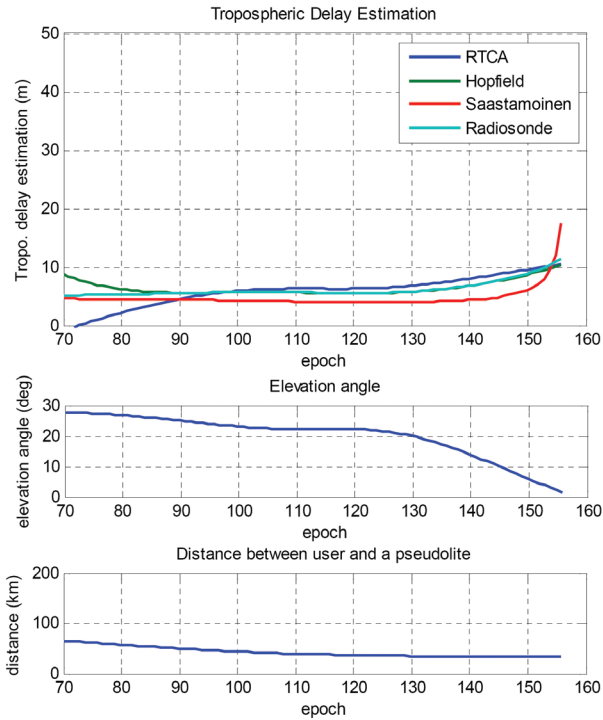
Fig. 6. Tropospheric delay estimation results of flight test case 2 (top: tropospheric delay estimation, middle: elevation angle between user and pseudolite, bottom : distance between user and pseudolite).

Fig. 7. Tropospheric delay estimation with respect to the distance between user and pseudolite.
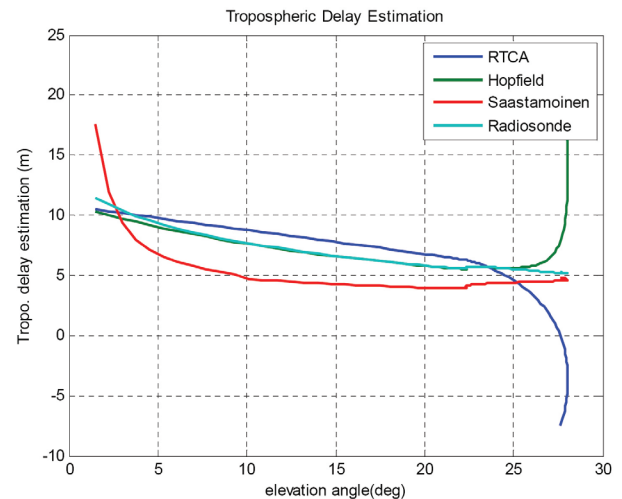
Fig. 8. Tropospheric delay estimation with respect to the elevation angle between user and pseudolite.

distance is reflected on the models, and thus their error is increased in proportion to the distance between them if the distance is increased or the height difference is increased. On the contrary, the Saastamoinen difference model showed the performance similar to that of the radiosonde observation data-based method, when the elevation angle was sufficiently high. When the elevation angle began to reduce at the epoch No. 130 and later, however, the Saastamoinen model showed a trend that was different from other models including the radiosonde-based model, as shown in Fig. 5.

Fig. 7 shows the tropospheric delay estimation result depending on the user receiver and the pseudolite. As the distance was 50 km or longer, the results of the RTCA model and the Hopfield model were significantly different from the radiosonde-based estimation. On the contrary, the trend of the Saastamoinen model was the same with that of the radiosonde-based estimation. Thus, the method to use a mapping function is the most effective when the distance between the user and the pseudolite is increased. The tropospheric delay estimation showed a significant change around the distance of 35 km, even though the distance was not changed a lot. In particular, the Saastamoinen model showed a great change, different from the other models, when the elevation angle was drastically decreased to 10
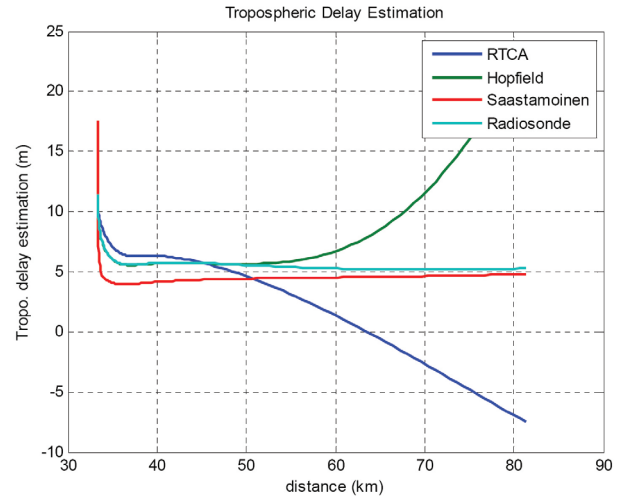
degree or less around the epoch No. 150 in Fig. 6. This indicates the limitation of the Saastamoinen model in the low elevation angle range.

Fig. 8 shows the tropospheric delay estimation performance depending on the elevation angle. The RTCA model and the Hopfield model showed a significant difference with the radiosonde-based model at the elevation angle of 25 or higher, which is the case where the distance was long as in the range of the epoch No. 80 or less in Fig. 6. When the elevation angle continued to increase, the Saastamoinen model approached the radiosonde-based model. When the elevation angle was significantly low, less than 5 degree, the Saastamoinen model showed a trend that was totally different from those of the RTCA model, the

Hopfield model and the radiosonde-based model.

4.4 The effect of tropospheric delay estimation error on navigation performance

In satellite navigation, the constellation of the satellite is relatively isotropic to the user, and thus locally correlated error factors, such as the meteorological conditions, are removed a lot as common error in the process of calculating the navigation solution. In the pseudolite navigation system in which the user is relatively close to pseudolites, however, the distance as well as the elevation angle difference between the individual pseudolite and the user is greatly dependent on the user location. So, the pseudorange errors caused by the tropospheric delay are less correlated with each other and they are reflected on the navigation error because they cannot be eliminated as common errors when calculating the navigation solution.

Fig. 9 shows the magnitude of the horizontal navigation error of the post-processed navigation solution obtained by applying the each of the tropospheric delay model to the pseudorange estimation acquired from the Case 2 flight test, with reference to the navigation solution calculated by applying the radiosonde-based method. Similar to the characteristics of the pseudorange error, the Saastamoinen model difference method showed the performance that is the closest to that of the radiosonde-based method, if the elevation angle was kept sufficiently high and the distance was long. When the distance was reduced after the epoch No. 150, the RTCA model and the Hopfield model showed the performance that was the most similar to that of the radiosonde-based method.

5. CONCLUSIONS AND FUTURE WORKS

In this study, we qualitatively compared the performance of the tropospheric delay models applicable to pseudolite. We carried out radiosonde meteorological observation to prepare the comparison reference, and proposed the path integration tropospheric delay estimation method based on the acquired data. On the basis of the flight test data, we compared the tropospheric delay estimation errors and analyzed the effect of the tropospheric delay error on the navigation solution of the pseudolite navigation system.

The experimental result showed that the Saastamoinen difference method had the performance that was the most similar to that of the radiosonde-based method when the distance was long and the elevation angle was kept to be
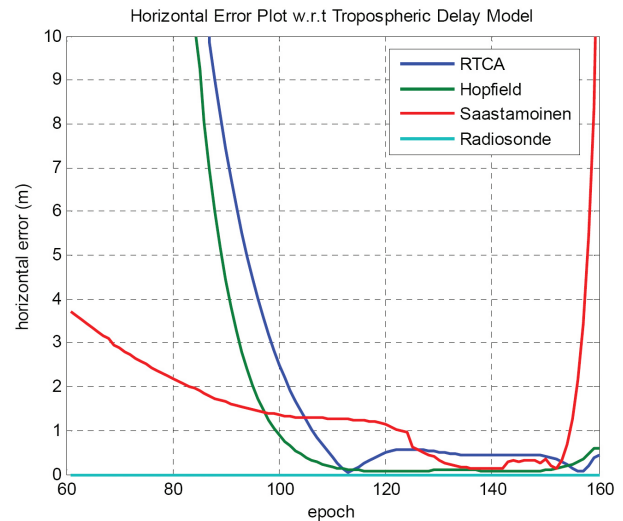

Fig. 9. Magnitude of Horizontal Navigation Error.

great sufficiently. When the elevation angle was small, however, a considerable error was induced. The RTCA model and the Hopfield model showed the performance similar to that of the radiosonde-based method if the distance is short, and thus they are considered as the most appropriate models for the condition. Based on the experimental results described above, we suggested that an appropriate tropospheric delay model could be chosen depending on the distance and elevation angle conditions between the flight and the pseudolite.

Each of the pseudolite tropospheric delay models compared and analyzed in this study showed the characteristics that are similar to the simulation results in the conventional studies. This is significant in the sense that the path integration method based on the radiosonde data, the reference data in this study, presented a meaningful reference values. As a future study, the error of the tropospheric delay models will be compared and analyzed quantitatively with reference to the radiosonde data-based path integration method under various meteorological conditions. On the basis of the result, we will propose a method to correct the error of the conventional tropospheric delay models under various meteorological conditions and flight trajectories.

ACKNOWLEDGMENTS

REFERENCES

Biberger, R., Teuber, A., Pany, T., & Hein, G. 2003, Development of and APL Error Model for Precision Approaches and Validation by Flight Experiments, in ION GPS/GNSS 2003, Portland, OR, USA, 9-12 Sep 2003

Bouska, J. & Raquet, F. 2003, Tropospheric Model Error Reduction in Pseudolite-Based Positioning Systems, in ION GPS/GNSS 2003, Portland OR, USA, 9-12 Sep 2003

Craig, D. & Locata Corp. 2012, USAF's New Reference System, Truth on the Range, in InsideGNSS Magazine, May/June 2012

Hofmann-Wellenhof, B., Lichtenegger, H., & Collins, J. 2000, GPS Theory and Practice, Springer, 5th ed. (New York: Springer-Verlag Wien)

Kaplan, E. & Hegarty, C. 2006, Understanding GPS Principles and Applications, 2nd Ed. (Boston: Artech House)

Kee, C., Yun, D., & Jun,H. 2003, Indoor Navigation System using Asynchronous Pseudolites, Journal of Navigation, 56, 443-455

Radio Technical Commission for Aeronautics (RTCA), 2000, GNSS Based Precision Approach Local Area Augmentation System (LAAS)-Signal-in-Space Interface Control Document, RTCA DO-246A

So, H., Lee, T., Jeon, S., Kim, C., Kee, C., Kim, T., & Lee, S. 2010, Implementation of a Vector-based Tracking Loop Receiver in a Pseudolite Navigation System, Sensors, 10, 6324-6346

Wang, J., Wang, J., Sinclair, D., Watts, L., & Lee, H. 2005, Tropospheric Delay Estimation for Pseudolite Positioning, Journal of Global Positioning System, 4, 106-111

Kiwon Song received the Doctor's degree in Electronicsfrom Chung-nam National University in 2002. His research interests include satellite navigation and GNSS signal processing.

Hyoungmin So is a senior researcher of Agency for Defense Development (ADD) in Korea, Republic of. He received B.S. degree in mechanical engineering at Korea Univ. and M.S. and Ph.D. degree in aerospace engineering at Seoul National University (SNU). He worked in the field of GNSS and pseudolite receiver development including SDR and vector tracking loop algorithm in SNU GNSS laboratory. Since 2011, he's been working for ADD.

Junpyo Park received his M.S. degree in Mechanical Engineering from the Busan National University in 1992. He is a Senior Researcher in the Agency for Defense Development, Korea. His research interests include integrity monitoring of GNSS signal, orbit determination, and GNSS-related engineering problems.